Mode-Selecting Micrograting Cavity Laser

Wen-Gang Yao, Kai-Min Guan, Zhen-Nan Tian, Jun-Jie Xu, Qi-Dai Chen, and Hong-Bo Sun, *Member, IEEE*

***Abstract*—We demonstrate a novel mode-selecting microcavity laser composed of gratings and a microdisk and fabricated by femtosecond-laser direct-writing technology. The microcavity laser shows good directivity and a single longitudinal mode, resulting from the mode coupling between the microdisk and gratings. The lasing wavelength can be regulated by adjusting the grating period. The properties of the laser were investigated and show good agreement with theoretical calculation and simulation. Based on the behavior and properties, this novel microcavity laser demonstrates good application prospects in integrated microoptics devices.**

***Index Terms*—Bragg grating, laser tuning, microstructure, microcavity laser, mode-selecting, photoluminescence, single mode, whispering gallery modes.**

I. Introduction

WHISPERING gallery modes (WGMs) were proposed by Lord Rayleigh in 1910, during a study on St. Paul's Cathedral. Microcavities, as a typical WGM structure, can limit and magnify light waves by continuous total internal reflection (TIR) along curved, smooth surfaces [1]. The small volume and high quality factor (Q-factor) of microcavities suggested significant potential applications in integrated micro-optics devices, such as optical filters [2], biological sensors [3], [4], light emitting devices [5] and quantum optics light sources [6]. The high processing performance and unique function of microcavity lasers have attracted significant attention in recent decades. A variety of microcavity structures have been proposed, such as microcolumns [7], microrings [8], [9], microdisks [10]–[12], and microtoroids [13], [14].

Wavelength tuning can be difficult in conventional semiconductor microcavities because of the intrinsic energy level structures of semiconductors. Dye-doped lasers may solve this problem because of the density of energy levels they offer. However, the dense energy levels result in a multiple-mode output spectrum, which greatly affects the monochromatic nature of the laser. To reduce redundant laser modes, many methods have been proposed. One classic technique selects a single mode from coupled cavities by means of the Vernier effect [15], [16]. For example, Shang *et al.* realized a single-frequency microcavity laser by coupling two asymmetric microcavities [17]. In another method, the cavities are reduced in size, causing the free spectral range (FSR) of a cavity to exceed the spectral width of the gain medium [18], [19]. Yu *et al.* acquired a single-mode laser-emission photoluminescence (PL) spectrum from a 4-μm-edge-length hexagonal microdisk [20]. A third method, optimal for achieving single-mode lasing, uses the design and fabrication of multilayered films or gratings with distributed Bragg reflection (DBR) or distributed feedback (DFB) structures [21], [22]. In a typical example, Nesnidal *et al.* developed a single-frequency, single-spatial-mode, large-aperture resonant-optical-waveguide (ROW)-DFB diode laser array [23]. Unfortunately, it is not plausible to select each available lasing mode, as these works are limited by the materials or methods utilized.

In this study, we demonstrate a novel grating/disk microcavity laser fabricated by femtosecond-laser direct-writing (FsLDW) technology. The significant coupling between the grating and microdisk caused a significant reduction in the miscellaneous output modes. The novel microcavity can achieve a single longitudinal mode with tunable capability, agreeing well with theoretical predictions. In addition, the emission laser showed good and stable directivity. The microcavity laser could be widely applied in integrated optical systems, especially in wavelength regulation and directional coupling occasions.

II. Theory and Experiments

In a WGM resonator, the light wave is trapped within the resonator by continuous TIR along a smooth curved surface. When the formula $2\pi nr = m \cdot \lambda_m$ (in which *n* is the refractive index of dye-doped resins with a value of $\sim$1.6, *r* is the radius of the disk, *m* is an integer, and λ_m is the *m-th* order resonant wavelength) is satisfied, standing light waves are formed; the energy of the wave is magnified to an ultra-high level by multiple-wave superposition.

The FSR refers to the difference between λ_m and λ_{m-1}, which depends on the radius of the resonator. For a general microdisk resonator with a diameter of 30 μm, many modes chosen by FSR can be output, which can seriously damage the monochromaticity of a microcavity laser.

To obtain a tunable single-mode microcavity laser, we designed a novel grating/disk structure shown in Fig. 1(b). When light is traveling in the cavity, the evanescent field of light exists within tens to hundreds of nanometers of the cavity's interface and can interact with the surrounding environment [24]. Thus the disk can easily couple with the gratings which serve as an optical filter allowing only waves of selected wavelength to go through. The selection rules could be defined by the optical grating equation $d \cdot n(\sin\theta_{\rm in} + \sin\theta_{\rm out}) = m' \cdot \lambda_{m'}$, where *d* is the length of the grating period; *n* is the refractive index of dye-doped resins with a value of $\sim$1.6; $\theta_{\rm in}$ and $\theta_{\rm out}$ are the angles of incidence and emergence, respectively, and equal to $\pi/2$ here; m' is the order of the grating; and $\lambda_{m'}$ is the selected resonant

Manuscript received April 23, 2016; revised July 02, 2016; accepted July 13, 2016. Date of publication July 17, 2016; date of current version August 12, 2016. This work was supported by the National Natural Science Foundation of China under Grants 61137001, 61590930, 91323301, 61435005, and 91423102.

The authors are with State Key Laboratory on Integrated Optoelectronics, College of Electronic Science and Engineering, Jilin University, Changchun 130012, China (e-mail: chenqd@jlu.edu.cn; Guankm1991@163.com; xiaotian86400@126.com; xu19090630@163.com; chenqd@jlu.edu.cn; hbsun@jlu.edu.cn).

Color versions of one or more of the figures in this paper are available online at http://ieeexplore.ieee.org.

Digital Object Identifier 10.1109/JLT.2016.2592101

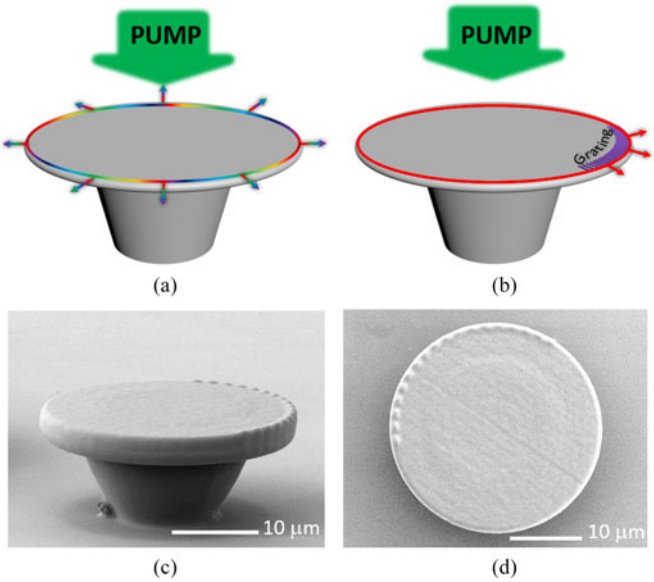

Fig. 1. Grating/disk microcavity laser. (a) Structural model of a disk cavity laser with homogeneous and various-modes emission. (b) Structural model of a grating/disk cavity laser with directional and single-mode emission. (c), (d) SEM images.

wavelength. The specific wavelength is selected only when the appropriate parameters (here, the length of the grating period) are satisfied.

The experiment is shown below. We chose the epoxy-based negative resin SU-8 2025 (MicroChem) diluted with cyclopentanone in a 1:1 volumetric ratio. Rhodamine B (RhB) dye, dissolved in ethanol to a concentration of 8% was added to the mixtures. The resulting dye-doped SU-8 resin contained a moderate amount of RhB at a concentration of 1 wt.%. The dye-doped resin was dip-coated on a glass substrate with a thickness of ∼1 mm for subsequent fabrication by FsLDW, following the procedures detailed here. The fabrication was performed on a three-dimensional displacement platform with an optic axial angle controlled by a system of two-dimensional scanning mirrors system; the height of the platform, parallel to the optical axis, was controlled through a piezoelectric micro-plate. High-intensity pulses from a femtosecond-laser oscillator (Tsunami, Spectra Physics) with a central wavelength of 790 nm, pulse width of 120 fs, and repetition rate of 80 MHz were tightly focused by a high-numerical-aperture (NA = 1.35) 100 × oil objective lens onto the prepared dye-doped resin. The designed grating/disk microcavity laser was obtained through spot scanning, set via two-photon polymerization.

Fig. 1(c) and (d) depict the top- and side-view scanning electron microscope (SEM) images of a grating disk microcavity, composed of a grating disk with a diameter of 30 μm and a thickness of 1.2 μm (top) and a 7-μm-high truncated conic base with an upper radius of 8.5 μm and a lower radius of 5 μm. One-third of the top surface edge of the disk is occupied by grating structures with a period of ∼1.6 μm.

The absorption band of the RhB-doped SU-8 occupies the range from 520 to 580 nm, so we selected a pumping light source with a wavelength of 532 nm provided by a doubling

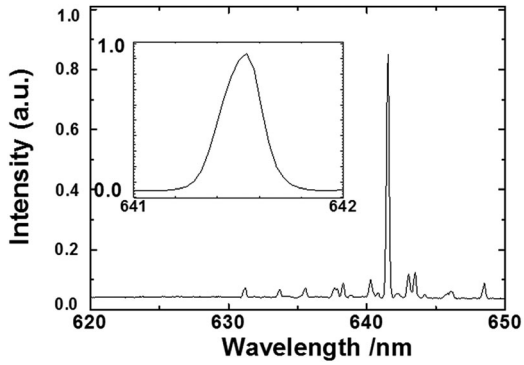

Fig. 2. One single-mode emission spectrum of the grating disk laser. Inset: magnification of emission peak.

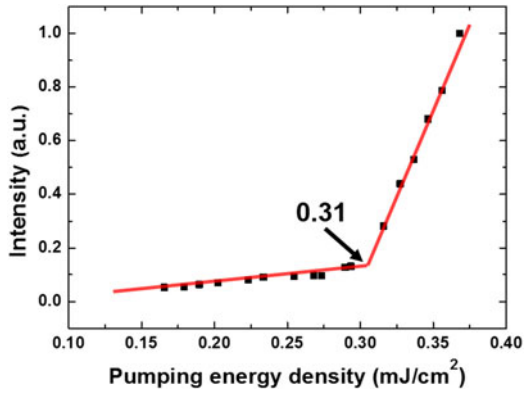

Fig. 3. Normalized intensity of emission light as a function of pumping laser power. The fitting curve illustrates a threshold as low as 0.31 mJ/cm^2.

crystal. The pumping picosecond laser had a pulse width of 15 ps, wavelength of 1064 nm, and repetition rate of 50 kHz. To obtain the accurate excitation threshold of the grating disk laser, a 20 × objective lens was added to the testing light path. The objective lens can focus the pumping light tightly onto the disk with a spot size of ∼50 μm which can be adjusted by changing the distance between the lens and the substrate. In addition, a charge coupled device (CCD) camera was used to maintain the position of the light spot in the experimental process. This permitted the acquisition of greater precision in measuring the excitation threshold.

III. Results and Discussion

In order to demonstrate the performance of the microcavity laser, we separately tested its monochromaticity, excitation threshold, directivity, and selectivity.

Fig. 2 depicts one stimulated emission spectrum of the grating disk with a period length of ∼1.6 μm. It shows a single-mode emission at ∼641.6 nm, close to the mode at ∼641.7 nm in the stimulated emission spectrum of a single disk without gratings, as shown in Fig. 5(a). The single-mode spectrum has a Q-factor of 2790, calculated according to Gaussian fitting. The inset of Fig. 2 shows a clear full width at half maximum of 0.23 nm.

To improve the accuracy of the measured threshold pumping power of the microcavity laser, we improved the testing system mentioned above and used a method that increased the pumping

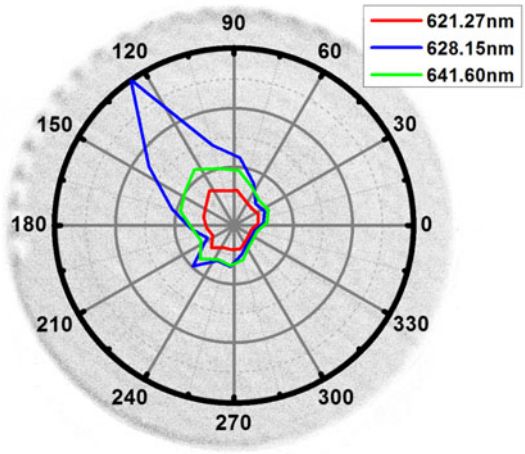

Fig. 4. Lasing intensity distribution of emission light from different angles; output direction coincides with relative position of gratings.

power and left other conditions unchanged. The fitting curve illustrates a threshold energy density as low as 0.31 mJ/cm^2, close to that of a microdisk cavity without gratings [25]. The result indicates that the gratings have very little negative effect on the stimulated emission.

The directionality of the laser eradiation was tested on a rotating 3D displacement platform, in which the detection head of the grating spectrometer has a permanent position, which ensures that the detection is in the same direction. Three microcavity lasers with various wavelengths were tested. They show good output directivity, as shown in Fig. 4. The output direction coincides well with the relative position of the gratings on the disk (the background image of Fig. 4), demonstrating that this optical device has a good relative-direction emission output. The mechanism of directional radiation may attribute to the coupling dissipation. When light wave is going through the gratings' field, the coupling dissipation provides much more possibility to emit than the field without gratings.

Fig. 5(a) shows a stimulated emission spectrum of a single disk with a diameter of $\sim$30 μm, which exhibits multifarious modes with an FSR of about 2.6 nm. When gratings are added to the disk, each mode can be selected individually. The mode-selection results are shown in Fig. 5(b–f). The five single modes with peaks at $\sim$636.1 nm, $\sim$637.9 nm, $\sim$641.6 nm, $\sim$644.5 nm, and $\sim$647.2 nm correspond, respectively, to the multimode peaks [see Fig. 5(a)] of $\sim$636.4 nm, $\sim$638.8 nm, $\sim$641.6 nm, $\sim$644.2 nm, and $\sim$646.9 nm, demonstrating the frequency selection ability within an allowable range of error. The multimode spectrum has an average Q-factor of 1280 which is much smaller than the Q-factor of 2790 of single-mode spectrum. This shows that gratings have the ability of narrowing peak shape to some extent.

In theory, for a grating period length of 1.61 μm, the grating would select the resonant wavelength of 642 nm, according to the optical grating equation with m' at the eighth order, which approaches the experimental result of 641.6 nm. We designed the 3D point-cloud data of the grating disk structure with a

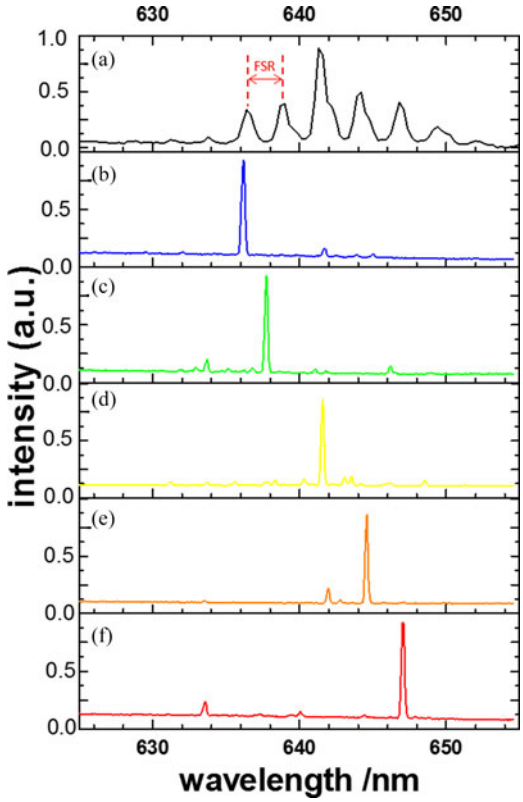

Fig. 5. Selected single-mode spectra of the grating/disk laser from a multimodal spectrum of a single disk laser. (a) Multi-modal spectrum of single disk laser. (b-f) Single-mode spectra of grating/disk microcavity laser, selected from spectrum (a).

grating period length of 1.6 μm using special software; the real length of the grating on the disk ranges from 1.5 μm to 1.7 μm because of systematic errors. The selection of emission output wavelengths is difficult to control under the current fabrication conditions. However, the frequency selection ability of the grating/disk structure has been demonstrated in reality. For further research, we will attempt to control the grating period using other substituting photoresists or optimizing the processing conditions.

IV. Calculation and Simulation

To further explain the mode-selection mechanism, a model based on coupled-mode theory of Bragg reflectors [26] has been proposed. In this model, the Eq. (1) is utilized to characterize the selection of the grating, which is illustrated with red lines in Fig. 6(a-d). The Eq. (1) is

$$R = \frac{\kappa^* \kappa \sinh^2 sL}{s^2 \cosh^2 sL + (\Delta\beta/2)^2 \sinh^2 sL} \tag{1}$$

given by Eq. (6.6–10) in the reference [26], where κ is the coupling coefficient, L is the length of the grating, s is given by $s^2 = \kappa^*\kappa - (\Delta\beta/2)^2$ and $\Delta\beta$ is the phase-mismatch factor. The black lines represent identical multimode spectra with a FSR of 2.6 nm, which were calculated, according to Eq. (2) of reference

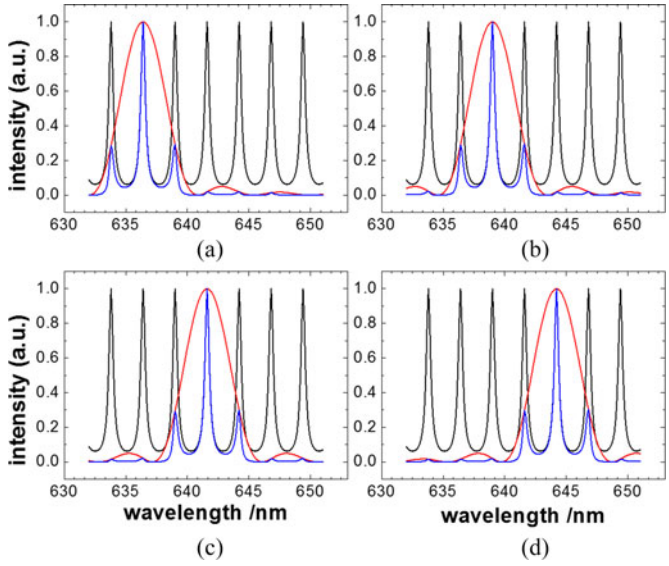

Fig. 6. Calculation diagram of mode-selection mechanism.

[27], by

$$D = \frac{1}{1 + \frac{4\Gamma^2}{(1-\Gamma^2)^2}\sin^2\left(\frac{n_g L\pi}{\lambda^2}\Delta\lambda\right)} \tag{2}$$

where $L = 2\pi R$ is the circumference of the disk, $n_g = \lambda^2/(L \cdot FSR)$ is the group refractive index, and Γ is sensitive to laser gain. The selected modes are illustrated with blue lines. The calculation results match well with the experiment results (Fig. 5) and the simulation results [see Fig. 7(a)].

In order to more vividly express the mode-selection mechanism of the grating, COMSOL Multiphysics simulation software was used to depict the progress of excitation light within the cavity based on the electric field intensity, using finite-element methods. A point magnetic dipole is added to the 2D grating/disk [see Fig. 7(b–d)] to imitate the pumping light with a frequency domain ranging from 4.65×10^{14} Hz to 4.91×10^{14} Hz; a point probe is used to detect the electric field intensity on the grating side. Fig. 7(a) depicts the simulated electric field intensity via the point probe; it demonstrates a much higher-intensity peak [peak 2 in Fig. 7(a)] compared to the side peaks [peaks 1 and 3 in Fig. 7(a)]. Fig. 7(b–d) depict electronic field intensity distributions of the grating/disk microcavity laser, corresponding to peak $1(4.7534 \times 10^{14}$ Hz), peak $2(4.7744 \times 10^{14}$ Hz), and peak $3(4.7974 \times 10^{14}$ Hz) in Fig. 7(a). Fig. 7(e–g) depict the respective enlarged views of the grating area.

The enlarged views of the electronic field intensity distributions near the grating area clearly demonstrate the frequency selection ability of the grating. Frequencies of 4.7534×10^{14} Hz and 4.7974×10^{14} Hz cannot easily cross the grating structure; thus, much more energy is lost, seriously restraining the formation of resonance oscillation. Only emissions at 4.7744×10^{14} Hz can cross the grating structure easily and form resonance oscillation. As a result, peak 2 is much higher in intensity than the other two peaks. In reality, the grating/disk is a 3D structure; when the light couples from the disk to the grating, it passes through air, which amplifies the energy loss. Non-selected frequencies, like those of peak 1 and peak 3, are weakened significantly, while the emission of peak 2 is relatively strengthened. Fig. 7(c) also illustrates that the emission intensity from the grating area is stronger than the other area.

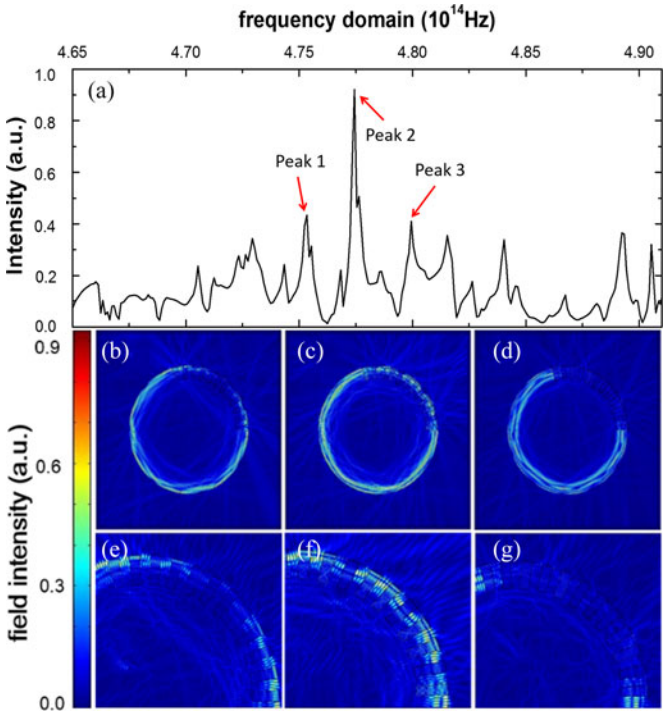

Fig. 7. COMSOL Multiphysics simulation of grating/disk laser. (a) Intensity spectrum of electric field via a point probe. (b), (c), (d) Intensity distributions of peaks 1, 2, and 3, respectively. (e), (f), (g) Enlarged views of grating area.

V. Conclusion

In conclusion, we have designed and fabricated a mode-selecting grating/disk microcavity laser. The laser has not only the ability of specific mode selection, but also the properties of directional emission output and low excitation threshold. The calculation and simulation clearly demonstrate the mechanism of the grating's mode selection. The proposed grating/disk laser offers one solution to wavelength tunability, significant in the development of functional integrated organic optoelectronic devices.

Acknowledgment

The authors would like to thank Xu-Lin Zhang from State Key Lab on Integrated Optoelectronics, Jilin University, for his help in simulation.

References

[1] K. J. Vahala, "Optical microcavities," *Nature*, vol. 424, no. 6950, pp. 839–846, Aug. 2003.

[2] B. E. Little *et al.*, "Ultra-compact Si-SiO_2 microring resonator optical channel dropping filters," *IEEE Photon. Technol. Lett.*, vol. 10, no. 4, pp. 549–551, Apr. 1998.

[3] F. Vollmer and S. Arnold, "Whispering-gallery-mode biosensing: Label-free detection down to single molecules," *Nature Methods*, vol. 5, no. 7, pp. 591–596, Jul. 2008.
[4] J. Su, A. F. G. Goldberg, and B. M. Stoltz, "Label-free detection of single nanoparticles and biological molecules using microtoroid optical resonators," *Light Sci. Appl.*, vol. 5, Jan. 2016, Art. no. e16001.
[5] C. Xiang, W. Koo, F. So, H. Sasabe, and J. Kido, "A systematic study on efficiency enhancements in phosphorescent green, red and blue microcavity organic light emitting devices," *Light Sci. Appl.*, vol. 2, Jun. 2013, Art. no. e74.
[6] A. J. Shields, "Semiconductor quantum light sources," *Nature Photon*., vol. 1, no. 4, pp. 215–223, Apr. 2007.
[7] J. M. Gérard, B. Sermage, B. Gayral, B. Legrand, E. Costard, and V. Thierry-Mieg, "Enhanced spontaneous emission by quantum boxes in a monolithic optical microcavity," *Phys. Rev. Lett.*, vol. 81, no. 5, Aug. 1998, Art. no. 1110.
[8] H. Hodaei, M. A. Miri, M. Heinrich, D. N. Christodoulides, and M. Khajavikhan, "Parity-time–symmetric microring lasers," *Science*, vol. 346, no. 6212, pp. 975–978, Nov. 2014.
[9] C. Zhang *et al.*, "Self-assembled organic crystalline microrings as active whispering-gallery-mode optical resonators," *Adv. Opt. Mater.*, vol. 1, no. 5, pp. 357–361, May 2013.
[10] X. Wang, Q. Liao, Q. Kong, Y. Zhang, Z. Xu, X. Lu, and H. Fu, "Whispering-gallery-mode microlaser based on self-assembled organic single-crystalline hexagonal microdisks," *Angew. Chem.-Int. Edit.*, vol. 53, pp. 5863–5867, Jun. 2014.
[11] K. J. Che, M. X. Lei, G. Q. Gu, Z. P. Cai, and Y. Z. Huang, "Optical processing between two metallically hybrid microdisks," *Appl. Opt.*, vol. 52, no. 23, pp. 8190–8194, Dec. 2013.
[12] J. F. Ku, Q. D. Chen, R. Zhang, and H. B. Sun, "Whispering-gallery-mode microdisk lasers produced by femtosecond laser direct writing," *Opt. Lett.*, vol. 36, no. 15, pp. 2871–2873, Aug. 2011.
[13] J. Li, S. Zhang, R. Yu, D. Zhang, and Y. Wu, "Enhanced optical nonlinearity and fiber-optical frequency comb controlled by a single atom in a whispering-gallery-mode microtoroid resonator," *Phys. Rev. A.*, vol. 90, no. 5, Nov. 2014, Art. no. 053832.
[14] D. K. Armani, T. J. Kippenberg, S. M. Spillane, and K. J. Vahala, "Ultra-high-Q toroid microcavity on a chip," *Nature*, vol. 421, no. 6926, pp. 925–928, Feb. 2003.
[15] E. Xu, Y. Sun, J. D. Suter, and X. Fan, "Single mode coupled optofluidic ring resonator dye lasers," *Appl. Phys. Lett.*, vol. 94, no. 24, Jun. 2009, Art. no. 241109.
[16] J. F. Ku *et al.*, "Photonic-molecule single-mode laser," *IEEE Photon. Technol. Lett.*, vol. 27, no. 11, pp. 1157–1160, Jun. 2015.
[17] L. Shang, L. Liu, and L. Xu, "Single-frequency coupled asymmetric microcavity laser," *Opt. Lett.*, vol. 33, no. 10, pp. 1150–1152, May 2008.
[18] K. H. Li, Z. Ma, and H. W. Choi, "Single-mode whispering gallery lasing from metal-clad GaN nanopillars," *Opt. Lett.*, vol. 37, no. 3, pp. 374–376, Jan. 2012.
[19] D. J. Gargas, M. C. Moore, A. Ni, S. W. Chang, Z. Zhang, S. L. Chuang, and P. Yang, "Whispering gallery mode lasing from zinc oxide hexagonal nanodisks," *ACS Nano*, vol. 4, no. 6, pp. 3270–3276, Apr. 2010.
[20] Z. Yu *et al.*, "Self-assembled microdisk lasers of perylenediimides," *J. Amer. Chem. Soc.*, vol. 137, no. 48, pp. 15105–15111, Nov. 2015.
[21] S. Kalusniak, S. Sadofev, S. Halm and F. Henneberger, "Vertical cavity surface emitting laser action of an all monolithic ZnO-based microcavity," *Appl. Phys. Lett.*, vol. 98, no. 1, Jan. 2011, Art. no. 011101.
[22] L. Chen, and E. Towe, "Nanowire lasers with distributed-Bragg-reflector mirrors," *Appl. Phys. Lett.*, vol. 89, no. 5, Aug. 2006, Art. no. 053125.
[23] M. P. Nesnidal *et al.*, "Single-frequency, single-spatial-mode ROW-DFB diode laser arrays," *IEEE Photon. Technol. Lett.*, vol. 8, no. 8, pp. 182–184, Feb. 1996.
[24] S. Yang, Y. Wang, and H. Sun, "Advances and prospects for whispering gallery mode microcavities," *Adv. Opt. Mater.*, vol. 3, no. 9, pp. 1136–1162, Mar. 2015.
[25] X. P. Zhan *et al.*, "Unidirectional lasing from a spiral-shaped microcavity of dye-doped polymers," *IEEE Photon. Technol. Lett.*, vol. 27, no. 3, pp. 311–314, Jan. 2015.
[26] A. Yariv and P. Yeh, *Optical Waves in Crystals*, New York, NY, USA: Wiley, 1983, pp. 188–353.
[27] J. Song *et al.*, "Thermo-optical tunable planar ridge microdisk resonator in silicon-on-insulator," *Opt. Express*, vol. 19, no. 12, pp. 11220–11227, Jun. 2011.

Wen-Gang Yao received the B.S. degree in physics from the College of Physics, Jilin University, Changchun, China, in 2014, where he is currently working toward the master's degree. His current research interests include the integrated organic optoelectronic devices and the transcription based on ion beam etching.

Kai-Min Guan received the B.S. degree in physics from the College of Physics, Jilin University, Changchun, China, in 2014, where he is currently working toward the Master's degree. His current research interest include the interaction between laser and materials.

Zhen-Nan Tian received the B.S. degree in physics from the College of Physics, Jilin University, Changchun, China, in 2007, where he is currently working toward the Ph.D. degree. His current research interests include the area of integrated optoelectronic devices and quantum chip.

Jun-Jie Xu received the B.S. degree in electronics science and technology from the College of Electronic Science and Engineering, Jilin University, China, in 2013, where he is currently working toward the Master's degree. His current research interests include the area of integrated organic optoelectronic devices.

Qi-Dai Chen received the B.S. degree in physics from the University of Science and Technology of China, Anhui, China, in 1998, and then received the Ph.D. degree in plasma physics from the Institute of Physics, CAS, Beijing, China, in 2004. He worked as a JST Postdoctoral Researcher in the Department of Physics, Osaka City University, Japan, from 2005 to 2006, and then as an Associate Professor in the College of Electronic Science and Engineering, Jilin University, China. In 2011, he was promoted as a Full Professor. His research interests include laser nanofabrication technology for micro-optics, semiconductor laser beam shaping and sub-wavelength anti-reflective microstructure. So far, he has published more than 130 scientific papers in the above fields, which have been cited for over 1100 times according to ISI search report.

Hong-Bo Sun received the Ph.D. degree from Jilin University, Changchun, China, in 1996. He worked as a Postdoctoral Researcher at the University of Tokushima, Tokushima, Japan, from 1996 to 2000, and then as an Assistant Professor in the Department of Applied Physics, Osaka University, Osaka, Japan. He became a Project Leader in 2001. In 2005, he became a Professor (Changjiang Scholar) at Jilin University. His research interests include laser micronanofabrication, and its application in microoptics, micromachines, microfluids, and microsensors. Dr. Sun was awarded by the Optical Science and Technology Society in 2002, and won an Outstanding Young Scientist Award issued by the minister of MEXT (Japan) in 2006.